The dynamics of coupled atom and field assisted by continuous external pumping

G. Burlak[a,*], O. Starostenko[b], and J.A. Hernandez[a]
[a] *Centro de Investigación en Ingeniería y Ciencias Aplicadas, Universidad Autónoma del Estado de Morelos, Cuernavaca, Mor. Mexico.*
[b] *Departamento de Física, Electrónica, Sistemas y Mecatrónica, Universidad de las Américas Puebla, Ex. Hacienda Santa Catrina Mártir, Cholula, Puebla, 72820, Mexico.*

Recibido el 30 de septiembre de 2005; aceptado el 27 de abril de 2006

The dynamics of a coupled system comprising a two-level atom and cavity field assisted by a continuous external classical field (driving Jaynes-Cummings model) is studied. When the initial field is prepared in a coherent state, the dynamics strongly depends on the algebraic sum of both fields. If this sum is zero (the compensative case) in the system, only the vacuum Rabi oscillations occur. The results with dissipation and external field detuning from the cavity field are also discussed.

Keywords: Two-level atom; driving Jaynes-Cummings model; vacuum Rabi oscillations.

Estudiamos la dinámica de un sistema acoplado de un átomo de dos niveles y un campo electromagnético quántico de cavidad asistidos por un campo electromagnético clásico externo continuo (modelo Jaynes-Cummings guiado). Cuando el campo de la cavidad inicialmente es preparado en un estado coherente, la dinámica depende fuertemente de la suma algebraica de ambos campos. Si este suma es cero (caso compensativo) en el sistema solo ocurren las oscilaciones de Rabi de vacío. También discutimos los resultados con disipación y desintonización del campo externo con respecto al campo de la cavidad.

Descriptores: Átomo de dos niveles; modelo Jaynes-Cummings guiado; oscilaciones de Rabi de vacío.

PACS: 32.80; 42.50; 42.50.

1. Introduction

The ability to create, manipulate, and characterize quantum states is becoming an increasingly important area of physics research, with implications for such areas of technology as quantum computing, quantum cryptography, and communications (see Refs. 1 to 4). Most research in quantum nonlocality and quantum information is based on the entanglement of two-level particles. One of the most interesting aspects of its dynamics is the entanglement between atom and field states. This essentially quantum mechanical property with no classical analog is characterized by the impossibility of completely specifying the state of the global system through the complete knowledge of the individual subsystem's dynamics.

The Jaynes-Cummings model [5] (JCM) for the interaction between a two-level atom and a single mode of the electromagnetic field holds a central place in the description of such interaction and provides important insight into the dynamical behavior of atom and quantized field. In driving JCM, the cavity field and driving field start to interact, which provides an opportunity to study directly the field dynamics at joint interaction with a two-level atom. Recently, it was shown that the effective coupling between an atom and a single-cavity field mode in JCM (driving JCM) can be drastically modified in the presence of a strong external driving field [6-8]. The important line of this direction is to use microcavities and microspheres for changing the features of atom-field interaction as a result of placing an atom or quantum dots in a microcavity (see Refs. 10 to 12).

The driven Jaynes-Cummings model for cases where the cavity and external driving field are close to or in resonance with the atom has been studied by several authors. Alsing, Guo and Carmichael [13] studied the Stark splittings in the quasienergies of the dressed states resulting from the presence of the driving field in the case where both fields are resonant with the atom. Jyotsna and Agarwal [14] studied the effect of the external field on the Rabi oscillations in the case where the cavity field is resonant with the atom, but the external field may be resonant or nonresonant. Dutra, Knight and Moya-Cessa [15] studied a similar model where the external field was taken to be quantized. Much attention was given to the limit of high-intensity of the driving field. Chough and Carmichael [16] studied the JCM with an external resonant driving field, and showed that the collapses and revivals of the mean photon number occur over a much longer time scale than the revival time of the Rabi oscillations for the atomic inversion. Gerry [17] studied the interaction of an atom with a quantized cavity field and the external classical driving field in the regime where an atom and classical fields are highly detuned.

The goal of the present work is to calculate the dynamics of an atom coupled to a cavity field assisted by continuous external pumping in the case when the initial field is prepared in a coherent state. The main result is the following: starting with a field's mode in a coherent state and with the atom in its upper state, the dynamics strongly depends on the algebraic sum of the amplitudes of the initial cavity field and the external field. If this sum is close to zero (the compensative case), only the vacuum Rabi oscillations occur in the system.

This paper is organized as follows. In Sec. 2, we discuss the equations of motion for a two-level atom coupled to the field in a cavity with the assistance of a continuous pumping

classical field. Section 3 presents results of a numerical study of the dynamics of the atom and field subsystems for the dissipative case, using the technique of the master equation. The behavior of the entropy and Fourier spectrum of oscillations is also studied. In the last section, we discuss and summarize our results.

2. Basic equations

Consider a two-level atom driven by a classical external field $(1/2)E_e\exp(i\omega_e t)+c.c.$ and coupled to a cavity mode of the quantized electromagnetic field. The Hamiltonian for the atom-cavity system (assuming $\hbar=1$) in the rotating-wave approximation (RWA) is given by

$$H=\frac{1}{2}\omega_0\sigma_3+\omega_a a^+a+g\left[\sigma^-a^++\sigma^+a\right]+\frac{1}{2}\left[\mathcal{E}\sigma^+e^{i\omega_e t}+\mathcal{E}^*\sigma^-e^{-i\omega_e t}\right], \quad (1)$$

where ω_0 is the atomic transition frequency, ω_a is the cavity frequency, $g=d(\omega_a/\hbar V\varepsilon_0)^{1/2}$ is the coupling constant between the atom and the cavity field mode (d is the atomic dipole matrix element for the transition, and V is the mode volume), $\mathcal{E}=E_e d$ is the coupling constant between the atom and the external classical field (E_e is the amplitude of the external field), a^+ and a are the creation and annihilation operators for the cavity mode $[a,a^+]=1$. In general, ω_0 , ω_a, and ω_e are different. To remove the time dependence in H, we use the operator $\exp[-i\omega_e t(\sigma_3+a^+a)]$ to transform to a frame rotating at the frequency ω_e. The Hamiltonian in the rotating frame (the interaction picture) is then

$$H_i=\frac{\Delta}{2}\sigma_3+g\left[\sigma^-a^+e^{-i\delta t}+\sigma^+ae^{i\delta t}\right]+\frac{1}{2}\left[\mathcal{E}\sigma^++\mathcal{E}^*\sigma^-\right], \quad (2)$$

where $\Delta{=}\omega_0-\omega_e$, $\delta=\omega_a-\omega_e$, $\sigma^{\pm}{=}(\sigma^x\pm i\sigma^y)/2$, σ_x, σ_y, σ_z are Pauli matrices. First we consider the resonant case when $\Delta=0$ and $\delta{=}0$. The case of non-zero detuning $\delta\neq 0$ is discussed in the second part. The resonant Hamiltonian ($\omega_a=\omega_0=\omega_e$) in the interaction picture has the form

$$H_{ir}=g\left[\sigma^-a^++\sigma^+a\right]+\frac{1}{2}\left[\mathcal{E}\sigma^++\mathcal{E}^*\sigma^-\right]. \quad (3)$$

Furthermore we use the following dimensionless variables $\tau{=}\omega_0 t$, $g/\omega_0{\to}g$, $\mathcal{E}/\omega_0{\to}\mathcal{E}$. If $\mathcal{E}=0$, then Eq. (3) describes the standard JCM, while the case $\mathcal{E}\neq 0$ corresponds to driving JCM. To obtain the solution to Eq. (3), we introduce the displacement operator $D(\gamma){=}\exp\{\gamma a^+-\gamma^*a\}$, $\gamma{=}\mathcal{E}/2g$, which allows us to rewrite Eq. (3) as follows:

$$H_{ir}=gD^+(\gamma)(\sigma^+a+a^+\sigma^-)D(\gamma), \quad (4)$$

where the identity

$$D^+(\gamma)(a^+,a)D(\gamma){=}(a^+{+}\gamma^*,a+\gamma)$$

is used. Establishing in (4) the Hamiltonian

$$D(\gamma)H_{ir}D^+(\gamma)=g(\sigma^+a+a^+\sigma^-)$$

and the state vector $\left|\widetilde{\psi}\right\rangle = D(\gamma)\left|\psi\right\rangle$, one obtains the Schrödinger equation as

$$i\frac{\partial\left|\widetilde{\psi}\right\rangle}{\partial\tau}=(\sigma^+a+a^+\sigma^-)\left|\widetilde{\psi}\right\rangle. \quad (5)$$

Now consider the case when the initial state of the field in the cavity is a coherent state $|\alpha\rangle$, with $\alpha{=}\overline{n}^{1/2}e^{-iv}$ ($\overline{n}$ is the average number of photons in the field, v is a phase of this state). Also we assume the atom is prepared in the excited state $|e\rangle$ ($|g\rangle$ is the ground state). The initial state vector $|\psi\rangle=|e\rangle|\alpha\rangle=|e\rangle D(\alpha)|0\rangle$ allows us to write for Eq. (5) the corresponding initial state vector $\left|\widetilde{\psi}\right\rangle$ as

$$\left|\widetilde{\psi}\right\rangle=D(\gamma)\left|\psi\right\rangle=|e\rangle D(\gamma)D(\alpha)|0\rangle=|e\rangle\left|\widetilde{\gamma}\right\rangle, \quad (6)$$

where $\widetilde{\gamma}{=}\gamma+\alpha$ and overall factor $\exp(i\Im(\gamma\alpha^*))$ is dropped. With Eq. (6), the solution to the standard JCM Eq. (5) is given by

$$\left|\widetilde{\psi}(\xi)\right\rangle=\sum_{n=0}^{\infty}C_n(\widetilde{\gamma})\{\cos(\xi\sqrt{n+1})|e\rangle|n\rangle - i\sin(\xi\sqrt{n+1})|g\rangle|n+1\rangle\}, \quad (7)$$

where $\xi{=}g\tau$, $C_n\equiv C_n(\widetilde{\gamma}){=}\exp(-|\widetilde{\gamma}|^2/2)\widetilde{\gamma}^n/\sqrt{n!}$ are expansion coefficients for the $|\widetilde{\gamma}\rangle$ state in the number representation $|n\rangle$. Equation (7) allows us to write the solution to resonant driving JCM (3) $|\psi(\xi)\rangle=D(-\gamma)\left|\widetilde{\psi}\right\rangle$ as follows:

$$|\psi(\xi)\rangle=\sum_{n=0}^{\infty}C_n(\widetilde{\gamma})\{\cos(\xi\sqrt{n+1})|e\rangle|-\gamma;n\rangle - i\sin(\xi\sqrt{n+1})|g\rangle|-\gamma;n+1\rangle\}, \quad (8)$$

where $|-\gamma;n\rangle=D(-\gamma)|n\rangle$ is the displaced number state. Note the following: formally, quantities $\mathcal{E}$ and α have different physical meanings $\mathcal{E}$ is used as a parameter of the driving field in the Hamiltonian (1), while α is a factor of the initial conditions for the field's mode in the cavity. However, the dependence of the probability coefficients $C_n(\widetilde{\gamma})$ on the combination $\widetilde{\gamma}=\mathcal{E}/2g+\alpha$ in (8) shows a deep similarity of these quantities (at least the resonant case $\delta=0$ considered here) since the coherent field state α has minimum uncertainty, and resembles the classical field as closely as quantum mechanics permits [18]. From Eq. (8), the density operator ρ can be written as follows:

$$\rho=|\psi(\xi)\rangle\langle\psi(\xi)| = |e\rangle\langle e|U_{ee}+|e\rangle\langle g|U_{eg}+|g\rangle\langle e|U_{ge}+|g\rangle\langle g|U_{gg}, \quad (9)$$

where matrix elements U_{ij} are given by

$$U_{ee}= \sum_{n,m=0}^{\infty} C_n^* C_m \cos(\xi\sqrt{m+1}) \times \cos(\xi\sqrt{n+1}) \left|-\gamma; m\right\rangle \left\langle -\gamma; n\right|, \quad (10)$$

$$U_{eg}= -i \sum_{n,m=0}^{\infty} C_n^* C_m \cos(\xi\sqrt{m+1}) \times \sin(\xi\sqrt{n+1}) \left|-\gamma; m\right\rangle \left\langle -\gamma; n+1\right|,$$

$$U_{eg}= i \sum_{n,m=0}^{\infty} C_n^* C_m \cos(\xi\sqrt{m+1}) \times \sin(\xi\sqrt{n+1}) \left|-\gamma; m+1\right\rangle \left\langle -\gamma; n\right|,$$

$$U_{gg}= \sum_{n,m=0}^{\infty} C_n^* C_m \sin(\xi\sqrt{m+1}) \times \sin(\xi\sqrt{n+1}) \left|-\gamma; m+1\right\rangle \left\langle -\gamma; n+1\right|,$$

and are still operators with respect to the field. To describe the evolution of the atom (field) alone, it is convenient to introduce the reduced density matrix

$$\rho^{a(f)} = Tr_{f(a)}\{\rho\}, \quad (11)$$

where the trace is over the field (atom) states. We have used the subscript a, f to denote the atom (field). Unlike the state vector, the density operator does not describe an individual system, but rather an ensemble of identically prepared atoms (see for example Ref. 19). A condition for the ensemble to be in a pure state is that $Tr\{\left(\rho^{a,f}\right)^2\} = 1$. In this case, a state-vector description of each individual system of the ensemble is possible. On the other hand, for a two-level system, a maximally mixed ensemble corresponds to $Tr\{\left(\rho^{a,f}\right)^2\} = 1/2$. Due to the identity

$$Tr_f\{\left|-\gamma; m\right\rangle \left\langle -\gamma; n\right|\} = Tr_a\{D^+(\gamma)\left|m\right\rangle \left\langle n\right| D(\gamma)\} = Tr_a\{\left|m\right\rangle \left\langle n\right| D(\gamma)D^+(\gamma)\} = \delta_{mn},$$

one can write ρ^a as follows:

$$\rho^a = \{\sum_{n=1}^{\infty} \left|C_{n-1}\right|^2 \left(\cos^2(\xi\sqrt{n})\left|e\right\rangle \left\langle e\right| + \sin^2(\xi\sqrt{n})\left|g\right\rangle \left\langle g\right|\right)\} + i\widetilde{\gamma}\{\sum_{n=1}^{\infty} \left|C_{n-1}\right|^2 \left(\cos(\xi\sqrt{n+1})\sin(\xi\sqrt{n})\left|e\right\rangle \left\langle g\right| - \sin(\xi\sqrt{n+1})\cos(\xi\sqrt{n})\left|g\right\rangle \left\langle e\right|\right)\}. \quad (12)$$

From Eq. (12), one can see that off-diagonal matrix elements $\rho^a_{eg}= \left\langle e\right| \rho^a \left|g\right\rangle$,and $\rho^a_{ge}= \left(\rho^a_{eg}\right)^+$ are of the first order with respect to $\widetilde{\gamma}=\gamma + \alpha$, $\gamma=\mathcal{E}/2g$, and therefore contain the information on the relative field's phase even in a weak field limit. The mean photon number $\langle n\rangle$ is given by

$$\langle n\rangle = \left\langle a^+ a\right\rangle_f = Tr\{a^+ a\rho^f\}. \quad (13)$$

Taking into account the identity

$$Tr\{a^+ a\left|-\gamma; m\right\rangle \left\langle -\gamma; n\right|\} = Tr\{D^+ Da^+ D^+ DaD^+(\gamma)\left|m\right\rangle \left\langle n\right| D(\gamma)\} = \left\langle n\right| (a^+ - \gamma^*)(a-\gamma)\left|m\right\rangle,$$

and after minor algebra, one may write (13) as follos:

$$\langle n\rangle = \left\langle a^+ a\right\rangle_f = A - B - B^*, \quad (14)$$

where

$$A = \left|\widetilde{\gamma}\right|^2 + \left|\gamma\right|^2 + \sum_{n=1}^{\infty} \left|C_{n-1}\right|^2 \sin^2(g\tau\sqrt{n}), \quad (15)$$

$$B = \frac{1}{2}\gamma\widetilde{\gamma}^* \sum_{n=1}^{\infty} \left|C_{n-1}\right|^2 \frac{1}{\sqrt{n}}\{Q_n^+ \cos\left[Q_n^- g\tau\right] - Q_n^- \cos\left[Q_n^+ g\tau\right]\}, \quad (16)$$

$$Q_n^{\pm} = \sqrt{n+1} \pm \sqrt{n},\ C_n = \exp(-\left|\widetilde{\gamma}\right|^2/2)\frac{\widetilde{\gamma}^n}{\sqrt{n!}},\ \widetilde{\gamma} = \gamma + \alpha = \frac{\mathcal{E}}{2g} + \alpha. \quad (17)$$

It is worth noting that in the field case considered, driving the coefficients A and B in Eqs. (15)-(16) depend on γ and $\widetilde{\gamma}$ separately. Therefore, the mean photon number $\langle n\rangle$ in Eq. (14) (with $\alpha \neq 0$) cannot be obtained by a simple shift from the mean photon number in the initially vacuum state ($\alpha = 0$).

We may observe that the quantum Rabi oscillations in (14) appear as the sum of the sinusoidal terms at incommensurable frequencies $g\sqrt{n}$, $gQ_n^{\pm}$, weighed by the probabilities $\left|C_n(\widetilde{\gamma})\right|^2$. One can see from Eqs. (12), (15)-(16) the following: since $\left|C_n\right|^2$ has a maximum at $n_m \sim \left|\widetilde{\gamma}\right|^2 = \left|(\mathcal{E}/2g) + \alpha\right|^2$ ($n > 1$), one may underscore the amplitude of specific Rabi oscillation in the spectrum of the excited-state probability $P^+(\tau)=\rho^a_{ee}$ (12) (the probability for the atom to be in the excited state) and $\langle n\rangle$ (14) by the adequate choice of the complex quantity $\mathcal{E}$. Simple calculation yields $n_m = E(\widetilde{\gamma}^2 - 1)$, where function $E(x)$ is the integer part of x. In an other interesting case, the external field $\mathcal{E}$ may be chosen as

$$\mathcal{E} = -2g\alpha. \quad (18)$$

In this case, in Eqs. (12), (14) the equalities $\widetilde{\gamma} = 0$, $B = 0$, $C_n = \delta_{n1}$ are fulfilled, so P^+ and $\langle n\rangle$ are reduced to the following simple form:

$$P^+ = \cos^2(g\tau) \text{ and } \langle n\rangle = \left|\frac{\mathcal{E}}{2g}\right|^2 + \sin^2(g\tau). \quad (19)$$

In this case, the two-level atom, which is initially in the excited state, undergoes the one-photon oscillations (radiating

and absorption of a photon), and only the vacuum Rabi frequency peak is present in the frequency spectrum. Note the Rabi oscillations for standard JCM were directly observed in Ref. 20.

The following experiment can be proposed on the basis of Eqs. (18)-(19). One can vary both amplitude and phase of the external field $\mathcal{E}$ until only a single vacuum Rabi frequency is observed in the spectrum. In this case the condition $\alpha = -\mathcal{E}/2g$ must hold, which provides the opportunity to measure parameters of the coherent state $|\alpha\rangle$. In the compensative case (18), these fields have equal amplitudes and frequency, but are shifted in phase by π.

The above analytical approach is valid in the case of very small dissipation (which describes the interaction of the atom and field subsystems with the environment) and zero detuning $\delta = 0$. But in the experiments, the damping of the cavity mode and the rate of spontaneous emission of the atom really are not small. Thus, a cavity damping must be included in a treatment of driving JCM to study the real dynamics and compare it with the experiments. An equation for the density operator $\rho(\tau)$ is required (master equation) because the loss of coherence due to the reservoir transforms any pure state into a mixture of states. With cavity damping in effect, we must solve a master equation for the joint atom-field density operator ρ of the two-level atom coupled to the electromagnetic field in the cavity. This equation is given by

$$\frac{d\rho}{d\tau} = -i[H_i, \rho] + \mathcal{L}_1\rho + \mathcal{L}_2\rho, \qquad (20)$$

with H_i given by (2). For the sake of simplicity, we consider only the case $\delta \neq 0$ and $\Delta = 0$, when the external field is not resonant to the cavity mode, which is an important case for the microcavities with the finite distance (frequency separations) between eigenfrequencies. The master equation (20) is more difficult to solve, and numerical methods usually need to be used. At interesting frequency ranges, the dissipation is written in Eq. (20) as mirror losses in the cavity that defines the mode of the electromagnetic field $\mathcal{L}_1\rho$, and as spontaneous emission from the atom $\mathcal{L}_2\rho$. At Born-Markov approximation and zero temperature, these parts are written in Eq. (20) as the following. One term is as follows: $\mathcal{L}_1\rho = \gamma_1 (2a\rho a^+ - a^+a\rho - \rho a^+a)$, where γ_1 is the rate of the single-photon losses. Another term $\mathcal{L}_2\rho = (\gamma_2/2)(2\sigma\rho\sigma^+ - \sigma^+\sigma\rho - \rho\sigma^+\sigma)$ takes into account the spontaneous emission from the atom out of the sides of the cavity [21]. In this case, the atom is damped by spontaneous emission with damping rate γ_2 to modes other than the privileged cavity mode with frequency ω_a. We have solved Eq. (20) numerically using truncated number states $|n\rangle$ and atom states $|e\rangle$, $|g\rangle$ basis. The algorithms for integration of such a system numerically can be found, e.g. in Ref. 22. In general $0 \leq n \leq \infty$, but for numerical calculations we have used $0 \leq n \leq M$. A finite basis of the number states M was kept large enough so that the highest energy state is never populated significantly. Since we assume previously that the field is initially in the coherent state $|\alpha\rangle$, and the atom is in the upper state $|e\rangle$, then initially $\rho = |\alpha\rangle\langle\alpha| \otimes |e\rangle\langle e|$ must hold. Using numerically obtained joint density matrix ρ, we have calculated the following quantities. Tracing out the matrix ρ over the field (atom) states, we calculated the reduced atom (field) density matrix $\rho^{a,f} = Tr_{f,a}\{\rho\}$, where $Tr_{a,f}\{\rho\}$ are the partial traces over the atom or field states accordingly. The latter allows us to study the dynamics of the excited-state probability $P^+(\tau) = \rho^a_{ee}$, the mean photon number $\langle n(\tau)\rangle$ and the entropy $S^a(\tau) = -Tr\{\rho^a \ln \rho^a\}$. Also the Fourier spectrum of $P^+(\tau)$ is explored. The convergence of the equations is tested and the dynamics of the system is studied for different values of the external field relative to the atom-field mode coupling. The results of the numerical solution of master equation (20) are shown in Figs. 1-4.

3. Numerical results

First we briefly consider the dynamics of the vacuum $\alpha = 0$ of driving JCM in order to understand some general features.

Figure 1 shows the evolution of the system for the resonant case ($\delta = 0$) for initial vacuum state $|0\rangle$ at losses case, obtained as a result of the numerical solution of the master equation (20). This solution is close to Eq. (12), but with a damping due to both mirror losses in the cavity and spontaneous emission from the atom. We use the following parameters: $\mathcal{E}$ =0.7, $g = 0.2$, $\gamma_1/\gamma_2 = 5$ and $\gamma_1 = 5 \cdot 10^{-3}$. To make the details of time evolution clearer, we have used the time interval $\tau = 200$, which is larger than the characteristic time scale of revival [23] $\tau > 2\tau_R$, where $\tau_R = 2\gamma\pi/g = 55$, $\gamma = \mathcal{E}/2g = 1.75$. Therefore, one can see that the dynamics of the probability of the excited level occupations $P^+(\tau)$ has the form of a damped sequence of collapses and revivals.

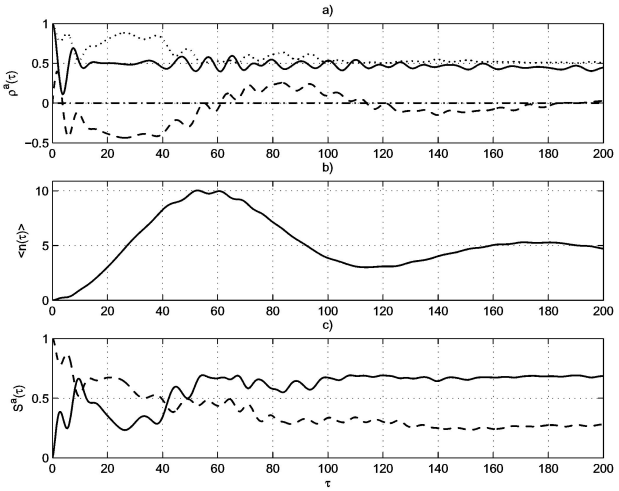

FIGURE 1. Quantum dynamics in driving JCM as a function of the interaction time τ for the initial vacuum case $|0\rangle$, $\delta = \Delta = 0$, $\mathcal{E} = 0.7$, $g = 0.2$, $\gamma_1 = 5 \cdot 10^{-3}$, $\gamma_2 = 10^{-3}$. (a) Probability of the excited level $|e\rangle$ occupations P^+ (solid line), $\Im(\rho^a_{ge})$ (dashed line), $Tr\{(\rho^a)^2\}$ (dotted line). (b) Mean photon number $\langle n\rangle$. (c) Entropy S^a (solid line), $Tr\{(\rho^f)^2\}$ (dashed line). See details in text.

Dynamical collapses and revivals are specific features of a unitary evolution. They are strongly affected by decoherency, which has the time constant set by the cavity field energy damping time $\sim 1/(\gamma_1+\gamma_2)$. From Fig. 1a, one can see that both collapses and revivals are progressively less pronounced due to dissipation $\gamma_{1,2} \neq 0$. The dissipation also reduces the magnitudes of non-diagonal elements ρ^a_{ge} (in this case $\rho^a_{eg} = (\rho^a_{ge})^*$ are purely imaginary quantities). One can see that the quantity $\Im(\rho^a_{ge})$ over time approaches zero due to losses, which causes the field phase information to wash out and hastens decoherence in the coupled system.

The dynamics $Tr\{(\rho^a)^2\}$ in Fig. 1a shows that in the collapse area the quantity $Tr\{(\rho^a)^2\}$ has a maximum close to 1 at $\tau_0 = \tau_R/2 = 27.5$. This point corresponds to the atomic attractor state which is completely independent on the initial atomic state [24]. At this point the compound system is in the disentangled state when in a lossless system $S^{a,f} \to 0$ and $Tr\{(\rho^{a,f})^2\} \to 1$. In lossy systems, such limit values are fulfilled only approximately. One can see from Fig. 1b that the mean photon number $\langle n\rangle$ increases from the initial zero value; however, over time $\langle n\rangle$ assumes the steady-state value justified by the amplitude of external driving field $\mathcal{E}$. Fig. 1c shows the dynamics of the entropy of the atom subsystem $S^a(\tau) = -Tr\{\rho^a \ln \rho^a\}$. In the area of the first collapse, S^a has an oscillating behavior. However, these oscillations are smoothed away over time and $S^a(\tau)$ approaches the steady-state value $ln(2) = 0.69$, which corresponds to a maximally entangled state of two-level atom and field mode. In a lossless case the exact equalities $Tr\{(\rho^a)^2\} = Tr\{(\rho^f)^2\}$ and $S^a = S^f$ fulfil the standard JCM [25]. This fact confirms our simulation with a high degree of accuracy.

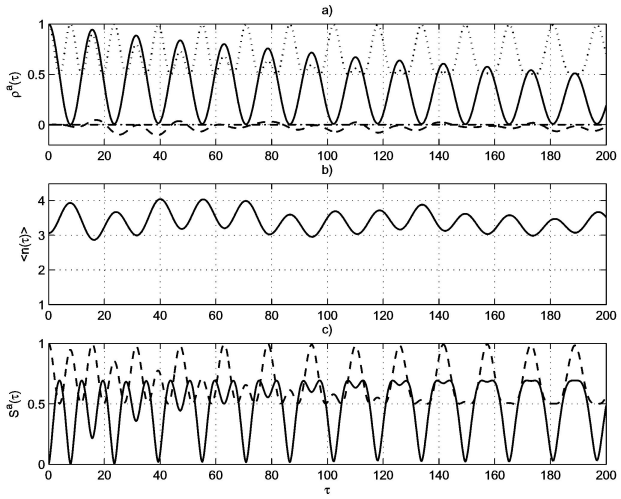

FIGURE 2. Quantum dynamics in driving JCM as a function of the interaction time τ for the initial coherent case $|\alpha\rangle$, $\alpha = -1.75$ (compensating case (18)), $\delta = \Delta = 0$, $\mathcal{E} = 0.7$, $g = 0.2$, $\gamma_1 = 5\cdot 10^{-3}$, $\gamma_2 = 10^{-3}$. (a) Probability of the excited level $|e\rangle$ occupations P^+ (solid line), $\Im(\rho^a_{ge})$ (dashed line), $\mathrm{Re}(\rho^a_{ge})$ (dash-dot line), $Tr(\rho^a)^2$ (dotted line). (b) Mean photon number $\langle n\rangle$. (c) Entropy S^a (solid line), $Tr(\rho^f)^2$ (dashed line). See details in text.

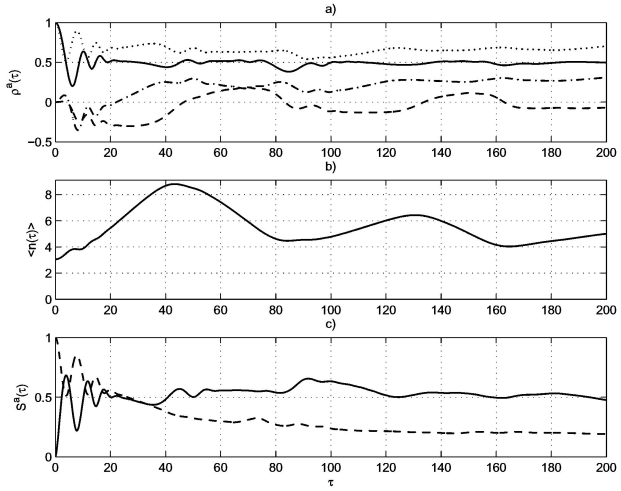

FIGURE 3. The same as in Fig. 2 but for detuning $\delta = 0.1$.

Next, we studied details of the driving and initial coherent field interaction. Fig. 2a shows the dynamics of the atom subsystem for the compensative case ($\widetilde{\gamma}$=γ+α=$\mathcal{E}/2g$+α=0) [see Eq. (18)] for the exact resonance case ($\delta = 0$)), but taking into account the dissipation $\gamma_{1,2} \neq 0$. A comparison of Fig. 2a and Fig. 2a shows that the dynamics for this case is essentially different from that of the initial vacuum case $\alpha = 0$ and has the form of damped vacuum Rabi oscillation in standard JCM.

The dynamics of the mean photon number $\langle n\rangle$ is of interest and is shown in Fig. 2b. The solid line in Fig. 2(b) shows results $\langle n\rangle$ from a numerical simulation of the atom-field master equation (20) for the compensative case, taking into account the losses in the system. For a short period of time $\tau < 10$, this simulation is in very good agreement with the exact formula (19). However a discrepancy arises over time due to losses not included in (19). One can see that, despite the mutual compensation of the initial coherent field and driving field in Eq. (19), the mean number of photons oscillates in the vicinity of $\sim |\alpha|^2$, which is justified by the field $|\mathcal{E}|$. One can see from Fig. 2c that, for a short time, the dynamics of entropy is similar to that of the vacuum case. However, over longer time intervals, the impact of dissipation becomes essential. Despite this dissipation at the time instances $\tau_k = \pi(2k+1)/2g$, $k = 0, 1...$ the entropy $S^a(\tau_k)$ is very close to zero, which implies the transition of the coupled atom-field system to the uncoupled pure state. At moments $\tau_k = \pi k/g$, the entropy has a value close to $\ln 2$, which corresponds to the maximum entanglement of the two-level atom and the field. Since the mean photon number does not vanish (see Fig. 2b), this dynamics is asymptotically stable.

Figure 3 shows the dynamics of the coupled subsystem in the compensative case ($\widetilde{\gamma} = 0$) when both dissipation $\gamma_1, \gamma_2 \neq 0$ and detuning $\delta \neq 0$ are non-zero. Notice in a non-resonant case ($\delta \neq 0$) the time dependence in the Hamiltonian (2) is not removed, and therefore the displacement operator transformation already does not allow a reduction of driving JCM to standard JCM. Compared to the case of

the exact resonance (Fig. 2), the sequential collapses and revivals now practically disappear over long periods of time; in Fig. 3a only the first collapse can be seen. Nevertheless, the maxima of $Tr\{(\rho^a)^2\}$ remain resolvable. One can see from Fig. 3c that during short periods of time $\tau < 7$ the behavior S^a is similar to that of the vacuum case (Fig. 2c). However, over longer periods of time the influence of decoherence becomes essential. The entropy quickly approaches its asymptotic value.

Figure 4 shows the Fourier spectrum for the cases of the driving JCM considered above. This spectrum, obtained by the Fourier transform of numerically calculated $P^+(\tau)$, exhibits well separated discrete frequency components, which are scaled as square roots of the successive integers. The spectrum in Fig. 4a corresponds to the time dynamics presented in Fig. 1a. One can see that the P^+ spectrum at the initial vacuum state $|0\rangle$ for the driving JCM case is similar to that in a standard JCM (without driving field $\mathcal{E} = 0$) at the initial coherent field $|\alpha\rangle$. Note that, for standard JCM, such peaks were observed experimentally in Ref. 20. The spectrum in Fig. 4a is rather similar to the spectrum shown in Fig. 2d of the experiment [20] for $\gamma = 1.77$. We can conclude that the vacuum case of driving JCM is similar to a standard JCM case with a coherent initial field, at least for the exact resonance. This conclusion reiterates the fact that the coherent field state is as close to the classical field as quantum mechanics permits [18]. Note that Fig. 4a shows that peak number 2 is the highest one. In this case $\widetilde{\gamma} = 1.75$; therefore, the calculated number of the highest peak is $E[\widetilde{\gamma}^2 - 1] = 2$.

Figures 4b-4d represent the compensative case (18) for the loss and detuning case. Fig. 4b shows the spectrum for the case $\delta = 0$; however, for losses, which are not small. One can see only the peak, which corresponds to $n = 0$, that is present in the Rabi spectrum. This spectrum in Fig. 4b corresponds to the measured spectrum shown in Fig. 2a in Ref. 20 for a nearly vacuum case (no injected fields). Thus, the

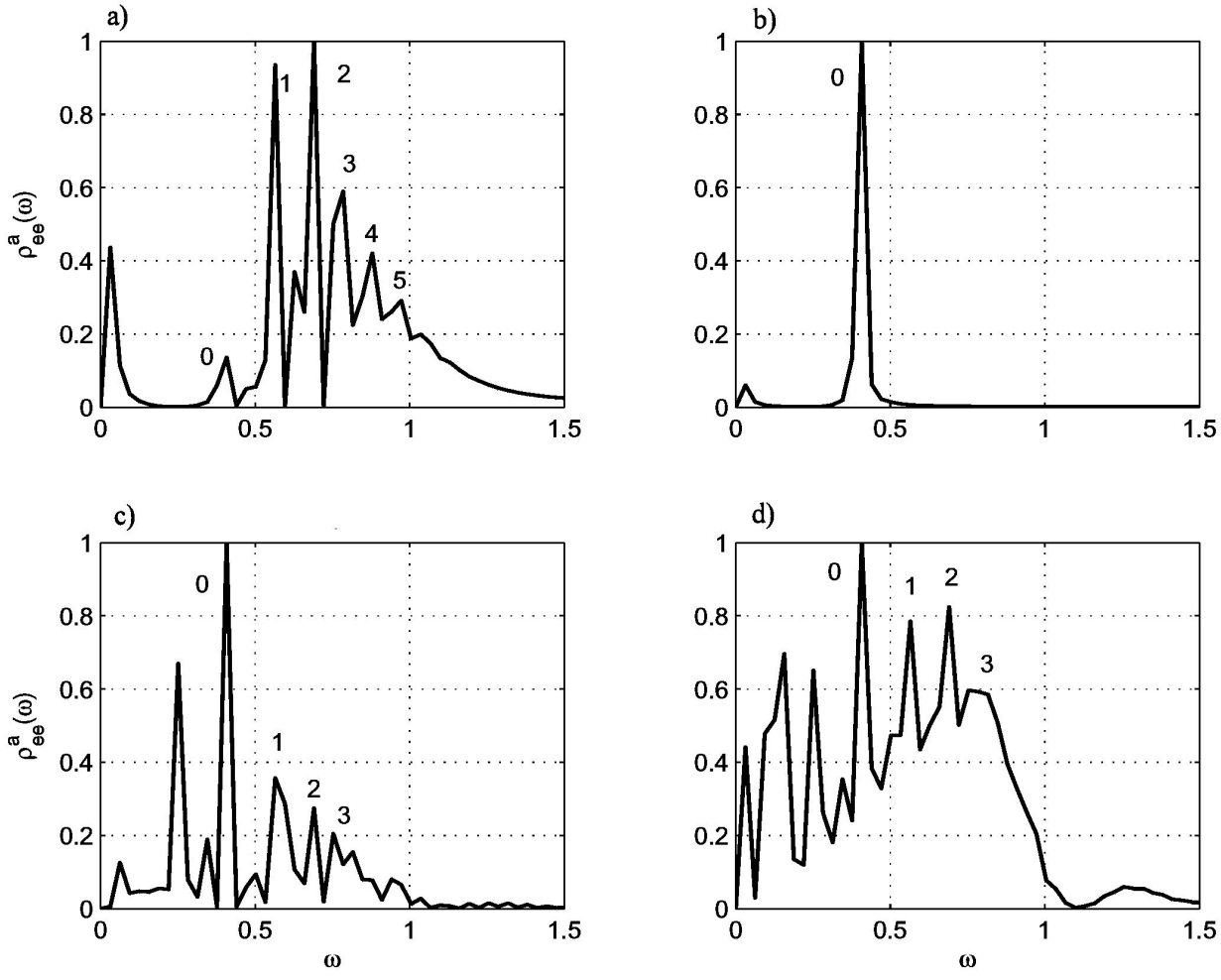

FIGURE 4. Fourier transforms of the probability $P^+(\tau)$ revealing the discrete Rabi frequencies, occurring at the successive square roots of the integers $\sqrt{n+1}$, numbers n=0, 1, 2... are inserted in the vicinity of peaks. Spectra correspond to a) Fig. 1a; b) Fig.2a; c) Fig. 3a, but with γ_1=$5 \cdot 10^{-5}$, γ_2=10^{-5}; d) Fig. 3a.

conclusion about the possible subtracting of the coherent and classical fields remains valid in the loss case also. In Fig. 4c, the influence of detuning is shown for smaller losses. One can see that even for case $\delta = 0.1$, which is not very small, the spectrum of several first Rabi frequencies is well recognizable. There are a few peaks in Fig. 4c, which correspond to detuning $\delta \neq 0$. Such peaks are present even at a larger dissipation rate (the dissipation rate in Fig. 4d is increased by two orders, with respect to Fig. 4c. Nevertheless the peak of vacuum oscillations remains dominant.

In general, one can readily derive that the quantity γ can be rewritten (with the previously used notations) as $\gamma{=}\mathcal{E}/2g{=}E_e/E_{vac}$, where $E_{vac}{=}(\hbar\omega_a/2\varepsilon_0 V)^{1/2}$ is the field per photon. Then from the equality $\widetilde{\gamma}{=}\gamma+\alpha{=}0$ (18), one can obtain $E_e = E_{vac}\overline{n}^{1/2}\exp(i(\upsilon+\pi))$. The latter equation shows that for the compensated case (18), the driving field E_e should be in a coherent state, but shifted by phase π concerning to initial state α. In general, the condition (18) does not hold exactly due to quantum fluctuations. However, since the ratio of fluctuation to the mean number (fractional uncertainty in the photon number, see for example Ch. 3 in Ref. 26 is $\Delta n/\overline{n} = \overline{n}^{-1/2}$ for a Poisson process, the larger the values of $\overline{n}$ become, the *higher* the accuracy of the condition (18).

4. Conclusion

The field-atom interactions in the driving JCM show that a variation of the amplitude or/and the phase of the driving field enables one to manipulate the dynamics and the spectrum of quantum Rabi oscillations. There are two distinct regimes. In the summarizing case of the driving field and the initial coherent field, one can underscore a selected frequency in the Rabi frequency spectrum. The subtraction provides the possibility of compensation of both fields. For the case of the exact compensation, the frequency spectrum of a two-level atom becomes similar to that of vacuum oscillations in standard JCM. Such processes may be useful in quantum information technology if the decoherence time is greater than the time scale of the atom-field interaction. In this case, these processes may have various applications related to monitoring the entanglement of the two-level atom with a quantized field, and may be used to develop quantum information technology devices.

Acknowledgements

The authors are grateful to Alexander (Sasha) Draganov (ITT Industries - Advanced Engineering & Science Division) who made several helpful comments. This work of G.B is partially supported by CONACyT grant 47220.

∗. Corresponding author: gburlak@uaem.mx

1. B.B. Blinov, D.L. Moehring, L.-M. Duan, and C. Monroe, *Nature*, **428** (2004) 153.
2. W.H. Zurek, *Rev. Mod. Phys.*, **75** (2003) 715.
3. J.M. Raimond, M. Brune, and S. Haroche, *Rev. Mod. Phys.*, **73** (2001) 565.
4. M. Brune, E. Hagley, J. dreyer, X. Maitre, A. Maali, C. Wunderlinch, J.M. Raimond, and S. Haroche, *Phys. Rev. Lett.* **77** (1996) 4887.
5. E. Jaynes and F. Cummings, *Proc. IEEE*, **51** (1963) 89.
6. E. Solano, G.S. Agarwal, and H. Walther, *Phys. Rev. Lett.*, **90** (2003) 027903.
7. S.-B. Zheng, *Phys. Rev. A.*, **66** (2002) 060303.
8. S.-B. Zheng, *Phys. Rev. A.*, **68** (2003) 035801.
9. P. Lougovski, F. Casagrande, A. Lulli, B.-G. Englert, E. Solano, and H. Walther, *Phys. Rev. A.*, **69** (2004) 023812.
10. K.J. Vahala, *Nature*, **424** (2003) 839.
11. M.V. Artemyev, U. Woggon, and R. Wannemacher, *Appl. Phys.Lett.*, **78** (2001) 1032.
12. G. Burlak, P.A. Marquez, and O. Starostenko, *Phys. Lett. A.*, **309** (2003) 146.
13. P. Alsing, D.-S. Guo, and H.J. Carmichael, *Phys. Rev. A.*, **45** (1992) 5135.
14. I.V. Jyotsna and G.S. Agarwal, *Opt. Commun.*, **99** (1993) 344.
15. S.M. Dutra, P.L. Knight, and H. Moya-Cessa, Phys. Rev. A., 54 (1993) 3168.
16. Y.T. Chough and H.J. Carmichael, *Phys. Rev. A.*, **54** (1996) 1709.
17. C.C. Gerry, *Phys. Rev. A*, **65** (2002) 063801.
18. R. Glauber, *Phys. Rev.*, **131** (1963) 2766.
19. J.-L. Basdevant and J. Dalibard, *Quantum mechanics* (Springer, 2002).
20. M. Brune, F. Schmidt-Kaler, A. Maali, J. Dreyer, E. Hagley, J.M. Raimond, and S. Haroche, *Phys. Rev. Lett.* **76** (1996) 1800.
21. M.O. Scully and M. Zubairy, *Quantum optics* (Cambridg,. University Press, 1996).
22. .H. Press, S.A. Teukovsky, W.T. Vetterling, and B.P. Flannery, *Numerical recipes in C++* (Cambridge, University Press, Cambridge, 2002).
23. N.B. Narozhny, J.J. Sanchez-Mondragon, and J.H. Eberly, *Phys. Rev. A.*, **23** (1981) 236.
24. J. Gea-Banacloche, *Phys. Rev. Lett.*, **65** (1990) 3385
25. S.J.D. Phoenix and P.L. Knight, *Phys. Rev. A.*, **44** (1991) 6023.
26. C. Gerry and P. Knight, *Introductory Quantum Optics* (Cambridge Uniersity Press, 2004).